Pore Formation During Solidification of Aluminum: Reconciliation of Experimental Observations, Modeling Assumptions, and Classical Nucleation Theory

PEDRAM YOUSEFIAN and MURAT TIRYAKIOĞLU

An in-depth discussion of pore formation is presented in this paper by first reinterpreting *in situ* observations reported in the literature as well as assumptions commonly made to model pore formation in aluminum castings. The physics of pore formation is reviewed through theoretical fracture pressure calculations based on classical nucleation theory for homogeneous and heterogeneous nucleation, with and without dissolved gas, *i.e.*, hydrogen. Based on the fracture pressure for aluminum, critical pore size and the corresponding probability of vacancies clustering to form that size have been calculated using thermodynamic data reported in the literature. Calculations show that it is impossible for a pore to nucleate either homogeneously or heterogeneously in aluminum, even with dissolved hydrogen. The formation of pores in aluminum castings can only be explained by inflation of entrained surface oxide films (bifilms) under reduced pressure and/or with dissolved gas, which involves only growth, avoiding any nucleation problem. This mechanism is consistent with the reinterpretations of *in situ* observations as well as the assumptions made in the literature to model pore formation.

https://doi.org/10.1007/s11661-017-4438-6

I. INTRODUCTION

ALUMINUM castings have been used in automotive and aerospace applications for their specific weight which helps with fuel efficiency. However, the mechanical properties and performance of aluminum castings are strongly affected by structural defects, such as pores and entrained oxide films,[1] which degrade tensile strength[2–5] and elongation[5–13] as well as fatigue life.[14–19] Moreover, pores can lead to rejection of the aluminum castings during final non-destructive inspection, such as X-ray. Moreover, pores have been observed[20] *in situ* to initiate hot tears, which are common in high strength cast aluminum alloys, such as the Al-Cu system. Therefore, understanding pore formation is paramount to lowering production costs, increasing their quality and performance, and consequently their wider use.

It is commonly assumed that pores nucleate in the last stages of solidification,[21] by shrinkage and/or rejection of dissolved gas by the solidifying metal. Consequently, pores have been characterized based on their appearance on micrographs, as either shrinkage or gas pores. Two examples are presented in Figure 1,[22] where the pore presented in Figure 1(a) has a tortuous shape because it is surrounded by the tips of dendrites and as a result, is usually interpreted as a shrinkage pore. The pore in Figure 1(b), however, is circular, and consequently, is interpreted as a gas pore. This interpretation is generally but not necessarily correct, as will be addressed later.

Because most aluminum castings have an abundance of pores, some researchers have stated that pores are intrinsic defects[23,24] and therefore cannot be eliminated. Whether pores are indeed intrinsic defects is addressed in this study, by reviewing and reinterpreting previous results of pore formation observations, common assumptions made in pore formation models, and the physics of pore formation. The differences between observations and the physics of pore nucleation are addressed *via* a review of the literature, and a mechanism that bridges the gap between physics and observations is discussed.

II. A REVIEW OF *IN SITU* OBSERVATIONS OF PORE FORMATION

Researchers have used a variety of methods to investigate pore formation during solidification, including

PEDRAM YOUSEFIAN and MURAT TIRYAKIOĞLU are with the School of Engineering, University of North Florida, Jacksonville, FL 32224. Contact e-mail: m.tiryakioglu@unf.edu
Manuscript submitted June 22, 2017.
Article published online December 17, 2017

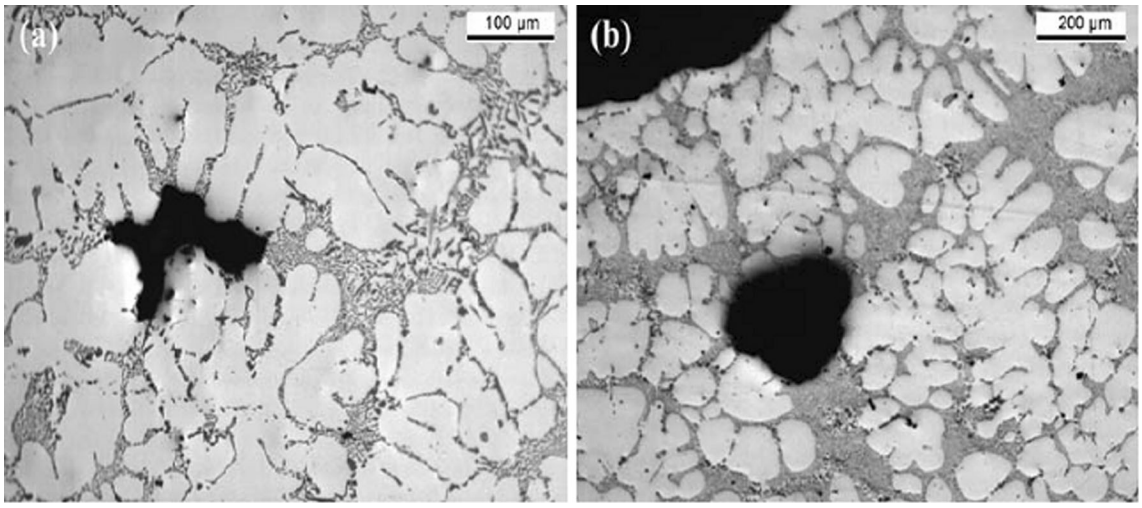

Fig. 1—Pores in a low-pressure die cast A356 engine block, commonly interpreted as a (*a*) shrinkage, and (*b*) gas pore (From ***Ref. [22] with permission).

- metallography of samples from castings after solidification,
- metallography of castings quenched while partially solidified,[25]
- *in situ* observation pores formed in transparent organic materials[26] with low melting points which behave similarly to metals, such as cyclohexane[27] and succinonitrile–acetone[20] with isothermal[28,29] and gradient[30,31] microscope stages
- *in situ* observation of pores in solidifying metals *via* X-rays

In this study, the results from the last group will be discussed.

In one of the earlier *in situ* studies using X-rays, Lee and Hunt[32] investigated pore formation in a directionally solidifying Al-Cu alloy. Four images from their observations are presented in Figure 2, in which a pore is indicated by an arrow. Note that the pore is not spherical and has a minor axis of approximately 0.2 mm. Non-spherical pores were also reported by Arnberg and Mathiesen[33] in their *in situ* study of solidification of an Al-30 pct Cu alloy using X-ray radiography. Yin and Koster[34] observed how pore shape evolves with solidification time in their study with pure aluminum. The X-ray radioscopic images of the pore observed by Yin and Koster are presented in Figure 3. The pore presented in Figure 3(a) is approximately 2 mm in diameter and appears near the solid–liquid interface when solid fraction, f_S, is 0.24. In Figure 3(b), the pore has grown in size to about 5 mm in diameter, maintaining its spherical shape, which becomes elongated in Figure 3(c), when the interfaces move. When the solidification is complete, the pore is not only elongated, but also has a tail, most probably due to liquid metal being sucked away due to solidification shrinkage. Yin and Koster attributed the pore formation to the supersaturation of hydrogen near the solid–liquid interface due to the rejection of hydrogen by solidifying aluminum. Similarly, Catalina *et al.*[35] also observed in an Al-0.25 wt pct Au alloy that a spherical pore formed away from the liquid–solid (S/L) interface and became elongated once it interacted with it.

Murphy *et al.*[36] conducted solidification experiments on a grain-refined Al-20 wt pct Cu alloy at very low cooling rates (0.084 K/s). Their observations at a solid fraction of 0.13 are presented in Figure 4. Note that spherical pores at $t = 91$ seconds are approximately 100 μm in diameter and they push the grains indicated (indicated in color) as they grow while maintaining their spherical shape.

Lei[37] studied pore formation during directional solidification of Al-7 wt pct Si and Al-12 wt pct Si alloys. They observed that pores appeared in the liquid at a distance of approximately 15 mm from the eutectic S/L interface, where the hydrogen supersaturation is usually expected to be quite low. Their results for the Al-7 wt pct Si alloy are shown in Figure 5. Note that pores have diameters as low as ~ 150 μm and are approximately spherical at $t = 75$ seconds. However, starting at $t = 90$ seconds, they progressively become tortuous, probably due their interaction with dendrites.

The results outlined above from *in situ* observations *via* X-rays in the literature show that pores can form (a) at a low solid fraction, (b) away from S/L interface, (c) usually as spheres, and (d) their final shape, *i.e.*, what can be observed on a metallographic section, such as the ones in Figure 1, cannot be used to describe how they have nucleated. Even whether pores can actually nucleate in aluminum has been questioned by Arnberg and Mathiesen[33] who suspected that only pore growth could be observed in *in situ* experiments. This hypothesis is supported by the findings of Kato[38] who investigated high purity copper in an atmosphere of H_2-Ar gas mixture. He observed that pores were formed heterogeneously on oxide films of aluminum and silicon when the hydrogen partial pressure in the atmosphere exceeded 0.3 atm. Hence, while pore formation was studied in

several studies, it remains unclear whether the actual nucleation of pores has ever been observed.

III. APPLICATION OF THE CLASSICAL NUCLEATION THEORY TO PORES IN CASTINGS

The physics of nucleation in condensed systems has been understood since the pioneering works of Völmer and Weber,[39,40] Becker and Döring,[41] and Gibbs.[42] The application of classical nucleation theory for pore nucleation has been addressed in several reviews.[43–49] The theory for pore nucleation will be summarized here. For more details, the reader is referred to the references above.

The simplest case of pore formation is homogeneous nucleation. Let us consider a pore nucleus with the external pressure, P_e, acting outside its surface. The external pressure will be the sum of the shrinkage pressure (P_s), the hydrostatic pressure due to depth (P_h), and the pressure applied to the surface of the liquid (P_{atm}). As a result, the amount of work (W) required to fracture the liquid to create a pore of volume V is equal to P_eV. There is, however, a surface energy barrier that needs to be overcome for the pore to be stable, which is equal to σA. The work to fill the pore with dissolved gas at internal pressure P_g is equal to $-P_gV$. The amount is negative because P_g helps the formation of the pore. Finally, the total work for the formation of the pore is:

$$W = \sigma A + V(P_e - P_g) \quad [1]$$

Assuming that pore nucleus is spherical and denoting ($P_e - P_g$) as ΔP, we have:

$$W = 4\pi r^2\sigma + \frac{4}{3}\pi r^3 \Delta P \quad [2]$$

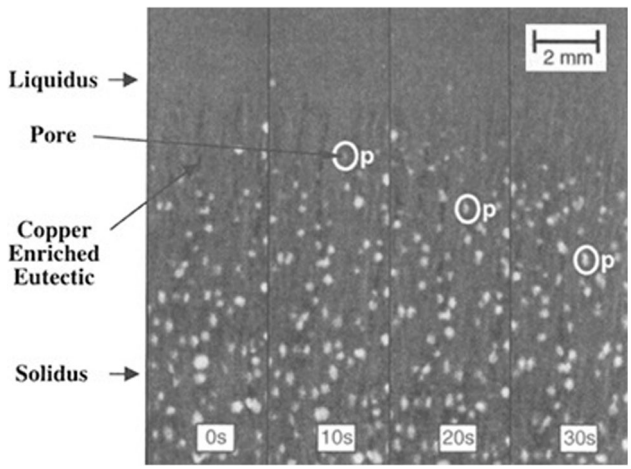

Fig. 2—Sequence of *in situ* X-ray radioscopic images of pore growth during solidification of an Al-Cu alloy. (From ***Ref. [32] with permission).

The schematic plot showing the effect of the two contributions to W as a function of pore radius is presented in Figure 6. Note that the critical radius above which a pore is stable, r^* is found by:

$$r^* = \frac{-2\sigma}{\Delta P^*}, \quad [3]$$

where ΔP^* is a negative number. Note that while surface energy for liquid metals is known, either ΔP^* or r^* needs to be estimated or alternatively assumed. Before the theoretical values based on classical nucleation theory are calculated, first assumptions made in the literature are presented.

IV. ASSUMPTIONS FOR MODELING PORE FORMATION

Over recent decades, significant effort has been made to model pore formation during the solidification process to help foundry engineers design industrial casting processes. These efforts range from analytical models and criteria functions to complex computational simulations.[50,51] As indicated above, these models need to assume either the critical radius or required pressure for pore formation as a nucleation criterion. Some of the assumptions made for modeling pore nucleation are summarized in Table I. Note that researchers[21,52–65] assumed either that there is no nucleation barrier to pore nucleation or critical radius as a set quantity related to microstructure, to model industrial casting processes accurately. The assumption frequently made that there is no barrier to nucleation means that the surface energy barrier to be overcome is zero, *i.e.*, no new surface is created during nucleation. Although this assumption has been shown to give accurate results for industrial processes, it is of course inconsistent with the principles of classical nucleation theory. This assumption is first compared to theoretical results based on classical nucleation theory.

V. FRACTURE PRESSURE OF LIQUID METALS

A. *Homogeneous Nucleation*

If a liquid is brought suddenly into a metastable state, a pore may appear spontaneously by nucleation and growth processes, and a phase separation takes place. Steady-state theories[39–41] of nucleation consider growth of clusters from a supersaturated vapor of single molecules by a series of reactions in which the clusters grow by addition of one molecule per reaction. The nucleation rate is then considered to be a product of the concentration of critical nuclei and the frequency with which they grow by addition of one molecule. A basic quantity, describing the kinetics of this process, is the steady-state nucleation rate, J, which is expressed commonly as[39,41,47,66]:

$$J = J_0 \exp\left(-\frac{W^*}{kT}\right) \quad [4]$$

Although Eq. [4] is universally accepted to be valid, the nucleation rate factor, J_0, has been interpreted differently among researchers. Fisher[66,67] estimated J_0 from the theory of absolute reaction rates to be

$$J_0 = \frac{N_A kT}{h} \exp\left(-\frac{\Delta G_0^*}{kT}\right) \quad [5]$$

Fisher stated that the rate of formation of bubbles of vapor in a mole of liquid subjected to a negative pressure P could be found by inserting Eq. [5] into Eq. [4]:

$$J = \frac{N_A kT}{h} \exp\left[\frac{-(\Delta G_0^* + W^*)}{kT}\right] \quad [4.a]$$

Fisher[67] then proceeded to introduce the fracture pressure of liquids, ΔP^*, based on the kinetics of phase transitions, as:

$$\Delta P^* = -\sqrt{\frac{16\pi\sigma^3}{3kT\ln\left(\frac{kN_A T}{h}\right)}} \quad [6]$$

The fracture pressure equation by Fisher provided close estimates for acetic acid and benzene.

Other researchers also attempted to develop similar equations for fracture pressure of liquids. Bankoff[68] modified Fisher's equation by considering a superheated liquid:

$$\Delta P^* = -\frac{\rho_l}{\rho_l - \rho_g}\sqrt{\frac{16\pi\sigma^3}{3kT\ln\left(\frac{6kN_A^{2/3}T}{h}\right)}} \quad [7]$$

Bernath[69] calculated ΔP^* by considering the frequency of nucleus formation which is a function of the molecular latent heat of vaporization, resulting in a cavity into which molecules may or may not vaporize:

$$\Delta P^* = -\sqrt{\frac{\frac{9.06\sigma^3}{kT}}{\ln\left(\frac{1.45\rho N_A^2\sigma^2}{\Delta P^* M^{3/2}\sqrt{kN_A T}}\right) - \frac{H_v}{kT}}} \quad [8]$$

The fracture pressure for homogeneous pore nucleation in pure aluminum at melting temperature and the corresponding critical radius (r^*) values calculated by Eqs. [6] through [8] as well as Eq. [3] are presented in Table I. The surface energy of liquid aluminum at melting temperature was taken as 0.914 J/m^2.[70] Note that these values are for liquid aluminum without dissolved gas or curvature effects. These assumptions will be revisited below.

Note that all equations give critical pore size results that are several orders of magnitude smaller than r^* assumed for modeling, Table II. Moreover, while pressure assumed for pore nucleation is consistently around zero in Table I, calculated fracture pressures are several gigaPascals. These theoretical values are 3 to 4 orders of magnitude higher than experimental tensile strength values reported in the literature (~ 1 MPa) for aluminum alloys at melting temperatures.[55,56] Hence, there is a significant discrepancy between the theoretical values and those assumed to have models that accurately predict pore formation. Moreover, it can be concluded that homogeneous nucleation of a pore in solidifying aluminum is impossible.

It is noteworthy in Table II that Fisher and Bankoff equations yielded very similar results and the Bernath equation gave a slightly lower value. The Bernath equation has been shown[69] to be accurate for a number of liquids at room temperature. Moreover, the fracture pressure of liquid lead was investigated[71,72] *via* molecular dynamics. Fracture pressure results were in the order of estimates provided by the three equations.[73] In addition, in an independent study, Martynyuk[74] used the modified Van der Waals equation to calculate the ideal tensile strength of metals, including aluminum, at melting temperature. Martynyuk found the ideal tensile strength of isotropic aluminum at melting temperature to be 4.80 GPa, which is closer to the values calculated by the Bankoff and Fisher equations for liquid aluminum at the same temperature. Hence, there is evidence in the literature supporting the accuracy of the level of theoretical fracture pressure for liquid aluminum.

In the absence of dissolved gas, the only mechanism available for a pore to nucleate is the formation of a vacancy cluster with a radius equal to r^*, because of the supersaturation of vacancies created during the solidification process.[75,76] The number of vacancies in the cluster with the critical pore size, n^*, is found by:

$$n_v^* = C_{AP}\left(\frac{r^*}{r_A}\right)^3 \quad [9]$$

C_{AP} is 0.74 for aluminum because of its face-centered cubic (FCC) crystal structure. Number of vacancies in the cluster with the critical pore size was calculated by inserting r^* in Eq. [9]. The number of vacancies needed in a vacancy cluster to form a pore with the critical size were calculated for the three fracture pressure equations. The results are presented in Table II, which show that large vacancy clusters are needed for fracture, *i.e.*, pore formation.

Brooks[77] derived an equation for the concentration, *i.e.*, probability of vacancy clusters with n_v vacancies, $P(n_V)$ as:

$$P(n_V) = \left[c_v \exp\left(\frac{E_V - (E_n/n_v)}{kT}\right)\right]^{n_v} \quad [10]$$

Jackson[78] calculated the formation energy of a vacancy (E_V) and spherical cluster of vacancy (E_n) as:

$$E_V = 12\sqrt{2}r_v^2\sigma \quad [11]$$

$$E_n = 15.36\, n^{2/3} r_v^2 \sigma \quad [12]$$

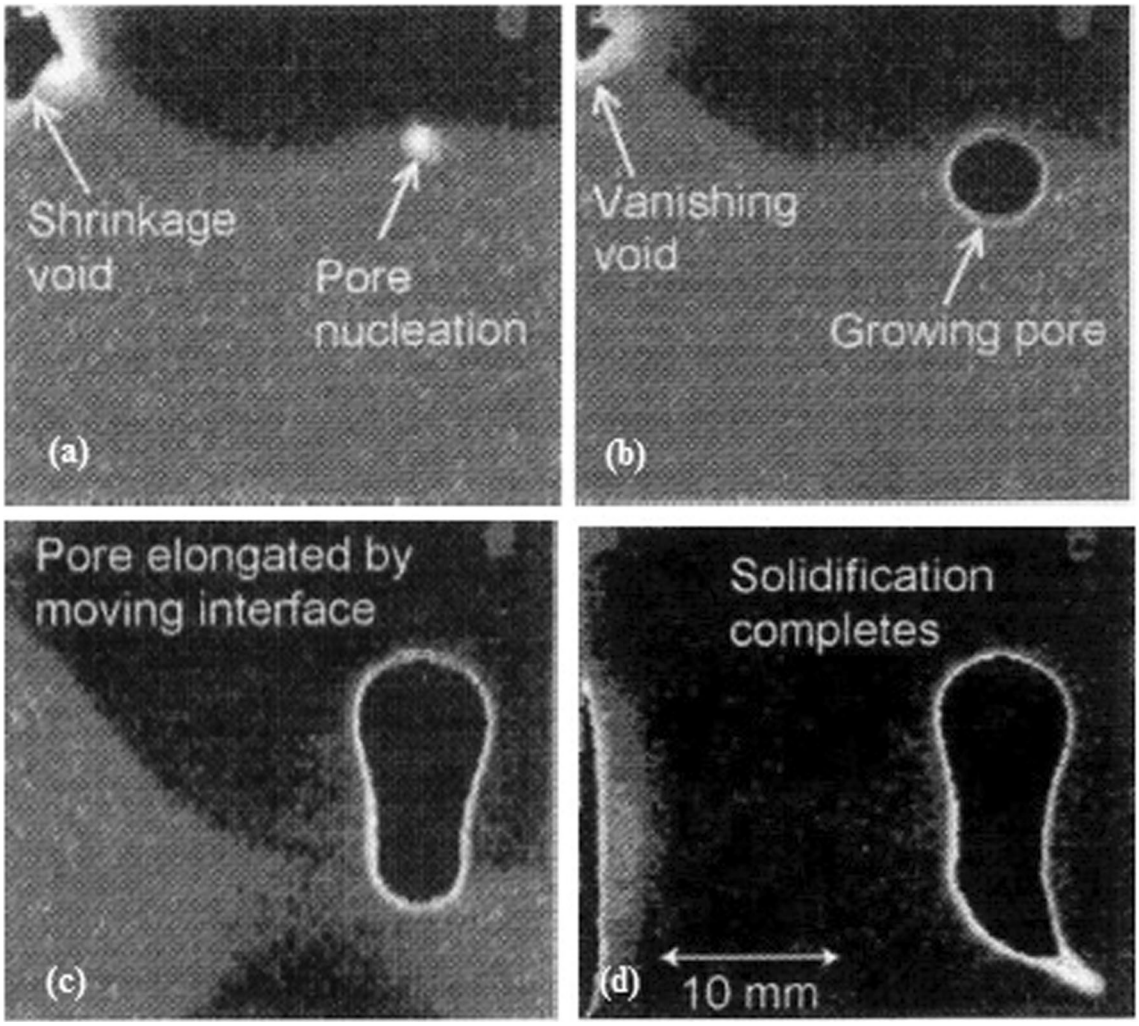

Fig. 3—Sequence of *in situ* X-ray radioscopic images of pore initiation and growth during solidification of pure aluminum (From ***Ref. [34] with permission).

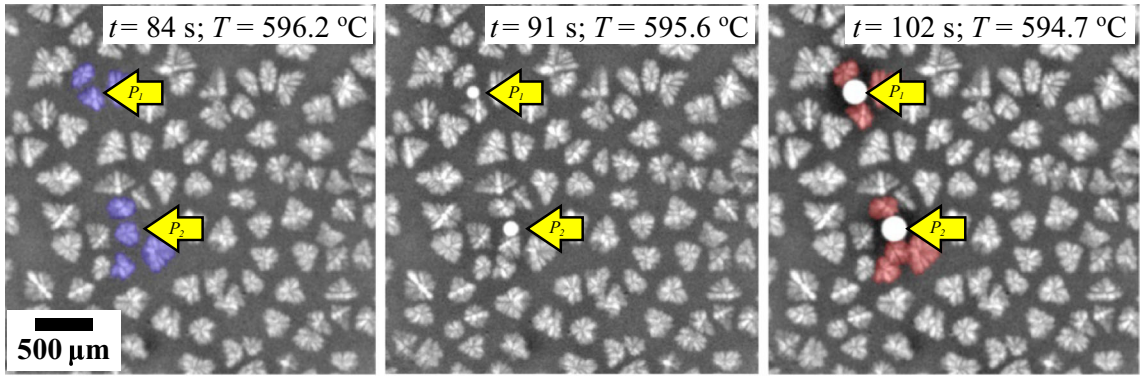

Fig. 4—The solidification of grain-refined Al-20 wt pct Cu sample. The locations of pores are indicated by arrows. Grains that were affected by the nucleation and growth of pores are indicated in color (From ***Ref. [36] with permission).

Thomas and Willens[79–81] conducted experiments to determine the vacancy concentration in liquid high purity aluminum (99.996 pct Al) by quenching from the liquid state. In these experiments, vacancies formed dislocation loops instead of voids, as also observed by Kuhlmann-Wilsdorf and Wilsdorf.[82] The change in vacancy concentration (c_v) in aluminum in liquid and solid states with temperature is presented in Figure 7. At

the melting point of aluminum, the equilibrium vacancy concentration is approximately 10^{-3}, which has been used as an approximation for all metals.[75]

By taking the radius of a vacancy in aluminum as 0.158 nm,[83] the equilibrium vacancy concentration at melting temperature to be 10^{-3}, the probability of a vacancy cluster with the size of a critical pore was calculated for the three fracture pressure equations using Eqs. [10] through [12]. The results are also presented in Table II. These results are extremely low probabilities, which lead to reaffirmation of the conclusion that homogenous nucleation of pores in pure aluminum without dissolved H is not possible.

B. *Effect of Curvature on Surface Energy*

In large vacancy clusters, the surface energy is simply the product of surface area and bulk surface energy as introduced in Eq. [2].[78] However, as the vacancy cluster gets smaller in size, the curvature effect will become increasingly more pronounced and will have a surface energy significantly less than a flat surface,[82,84] especially if the number of vacancies in the cluster is less than 40.[85] In the limit, if the radius of curvature of the surface is zero there is no surface, so the surface energy is zero. Si-Ahmed and Wolfer[86] showed that the effect of curvature on surface energy to form a vacancy cluster can described as

$$W_s = 4\pi r^2 \sigma \left[1 - \frac{0.8}{n_v + 2}\right] \qquad [13]$$

Hence effective surface energy can be written as:

$$\sigma_{\text{eff}} = \sigma \left[1 - \frac{0.8}{n_v + 2}\right] \qquad [14]$$

Subsequently, the critical pore size can calculated by effective surface energy into Eq. [3], in both numerator and denominator. The results presented in Table III show that curvature effects reduce fracture pressure values slightly but have essentially no effect on the critical pore size. Therefore, the conclusion that homogenous nucleation of pores in aluminum during solidification is impossible remains unchanged. This conclusion is consistent with the theoretical calculations of Zinkle *et al.*[76] who showed that pores were not favored in aluminum, and even if they form, they collapse into more stable, fully condensed, forms, such as loops and stacking-fault tetrahedrons.

C. *The Effect of Dissolved Gas*

The effect of gases dissolved in liquid metal on pore formation can be considered in two ways; (i) affecting stability of pores by changing the surface energy of solidifying metal, and (ii) increasing internal pressure in liquid. These aspects will be addressed in this section for liquid aluminum.

Hydrogen is the only gas with any significant solubility in liquid aluminum. The solubility of hydrogen is approximately 7 mL/kg in liquid and 0.4 mL/kg in solid state at melting temperature.[87] It is often speculated in the literature that the large difference in the solubility of H in liquid and solid states is the main reason for porosity in aluminum castings. The 7 mL/kg equilibrium concentration of hydrogen in liquid aluminum at melting temperature corresponds to approximately 1 atomic part per million (appm)[88] which is three orders of magnitude lower than that of vacancies. Hence, formation of vacancy clusters is still the required nucleation mechanism for pores, with dissolved gas only increasing the stability of pores and driving their growth.[89]

As stated in the last section, theoretical calculations showed that pores are metastable in aluminum, although several researchers[90–94] reported observing pores in pure aluminum samples quenched from high temperatures [~ 1000 K (727°C)] at high cooling rates (~ 10^4 K/s). It was speculated[76] that impurity atoms such as dissolved hydrogen can increase the stability of pores and therefore pores do not collapse to form loops or stacking-fault tetrahedrons. Obviously, the high cooling rates used in these studies are much higher than the ones in castings, and therefore results obtained from thin films cannot be directly applied to aluminum castings.

There is evidence provided in the literature[89,95–101] that suggest that surface energy can be reduced as much as 50 pct by the presence of dissolved gases. To determine what the effect of such a reduction would be, surface energy with dissolved gas, σ_g, was changed systematically from 0.914 J/m^2, the bulk surface energy of liquid aluminum, to 50 pct of that value. Fracture pressure, critical pore size, and number of vacancies in the initial cluster were calculated using Eqs. [6], [3], and [9], respectively. Results, indicated with subscripts "g" were normalized by taking ratios of calculations in the presence of gas to those without dissolved gas. The effect of reduction in surface energy on fracture pressure, critical pore size, and number of vacancies are presented in Figure 8. Although a decrease in surface energy should reduce the fracture pressure, the final result will be a larger critical pore size, and consequently a higher number of vacancies in the cluster and a lower probability of its formation. Therefore, any reduction in surface energy due to dissolved gas, such as hydrogen in aluminum, only serves to make homogeneous nucleation more difficult.

The second effect of dissolved hydrogen stated widely in the literature is its effect on the overall pressure, based on the assumption that aluminum goes from equilibrium solubility in liquid to solubility in solid instantaneously upon freezing. It is assumed that pressure buildup from rejected hydrogen atoms will add to the hydrostatic pressure of contraction to be sufficient to nucleate a pore.[102,103] Thus, the pore will nucleate when the effective pressure exceeds the fracture pressure of the liquid, followed by rapid growth of the pore, as observed in *in situ* experiments outlined above.

Because the solubility of hydrogen in liquid aluminum is approximately 20 times that in solid at melting temperature, excess hydrogen is expected to build up in

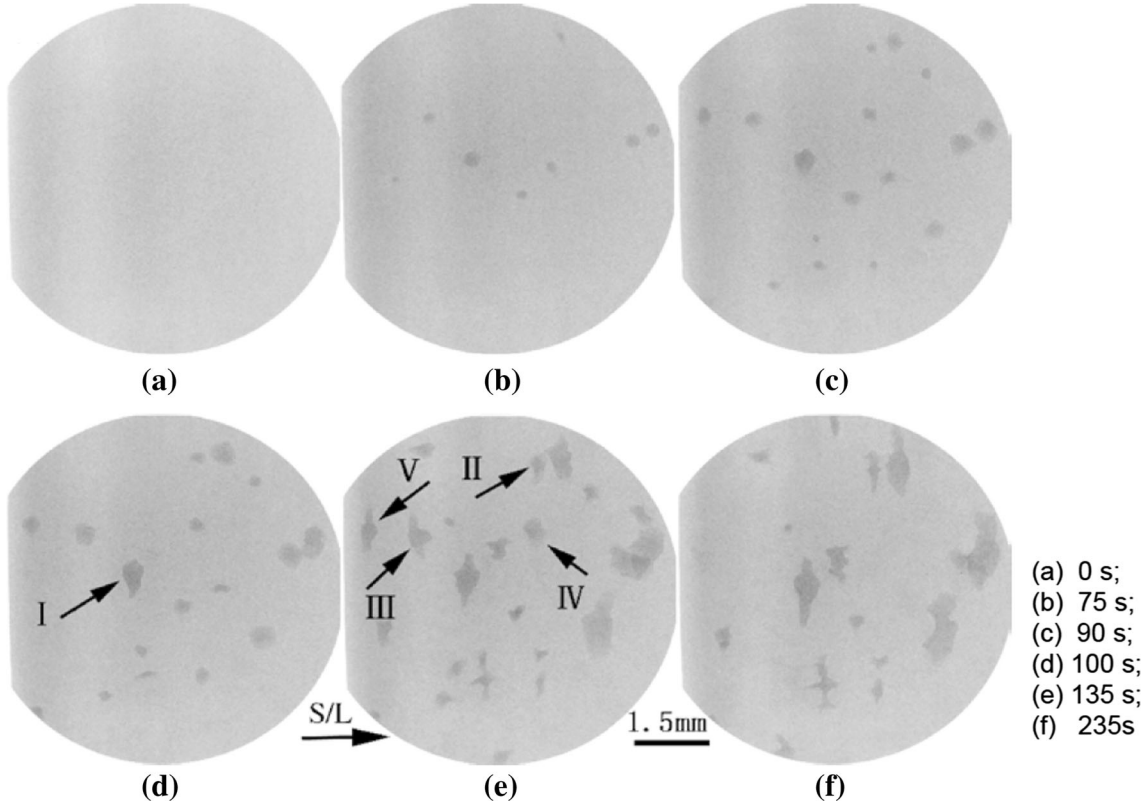

Fig. 5—The solidification sequence of an Al-7 wt pct Si sample. Pores are almost spherical at $t = 75$ s but they become increasing irregular with increasing time (From ***Ref. [37] with permission).

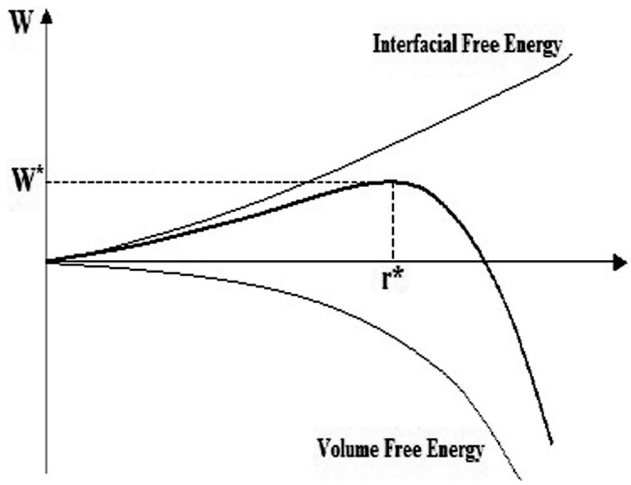

Fig. 6—Schematic plot of total work for pore nucleation as a function of pore radius.

intercellular and interdendritic channels. Piwonka and Flemings[21] hypothesized that this supersaturation can be as high as 100 times the solubility of hydrogen in liquid. To test the hypothesis of Piwonka and Flemings, the *in situ* experiments by Murphy *et al.*[36] were revisited. The vicinity of the first pore, designated as P_1, in Figure 4 at $t = 84$ seconds is presented again in Figure 9(a). The area designated by the box between the two cells between where the pore forms later is taken as the control volume. In Figure 9(b), the digital version of the box is presented with solid indicated in black and liquid in white. Digital image analysis showed that the local solid fraction is 0.434. Using the equilibrium solubility of hydrogen in liquid and solid provided above, the concentration of hydrogen in the liquid between the two cells can be estimated to be 1.73 times the equilibrium amount. Consequently, based on Sievert's law, the partial pressure of hydrogen can be calculated as 3 atmosphere or 3×10^{-4} GPa, which is four orders of magnitude less than the fracture pressure. Moreover, it is visible in Figure 4 that the pore that forms pushes the cells as it expands. Therefore, there is no physical constraint in the area where the pore forms. Based on these results, it can be concluded that the pore in Figure 4 did not nucleate homogeneously due to increased pressure from hydrogen supersaturation.

The discussion presented in this section clearly demonstrates that homogeneous nucleation of pores in aluminum solidifying at rates common in industrial castings is impossible. In the next section, heterogeneous nucleation will be addressed.

D. *Heterogeneous Nucleation*

In this section, whether pore nucleation is possible on certain types of preexisting solid surfaces which are poorly wetted such as non-metallic inclusions will be

Table I. Assumptions Made in Literature for Modeling Pore Nucleation

Pore Nucleation Criteria			
ΔP^*	r^*	References	Notes on Other Assumptions
= 0	n/c[1]	21	
n/c	$\lambda_{DA}/2$	52, 53	
n/c	$\lambda_{DA}/2$	54, 115	minimum supersaturation required for pore nucleation
n/c	1 μm	55	
~ 0	n/c	56	pores nucleate when the pressure in mushy zone is greater than the sum of the metallostatic head of the riser and the atmospheric pressure
n/c	n/c	57	nucleation occurs when hydrogen supersaturation is higher than 0.1 cc/100 g
n/c	n/c	58 through 60	empirically fitted stochastic distribution of pores based on supersaturation
= 0	half of cell size (5 through 10 μm)	61, 62	
n/c	= 10 μm	63	pore nucleation is not considered
= 0	n/c	64, 65	pores nucleate by gas supersaturation at heterogeneous nucleation site

[1]Not considered.

Table II. Fracture Pressure, Critical Size of a Nucleation Pore, Number of Vacancies in the Cluster, and the Probability of Formation of that Vacancy Cluster Calculated for Pure Solidifying Aluminum Without Dissolved Gases or Curvature Effects

Equation	ΔP^*(GPa)	r^* (nm)	n_v^*	$P\ (n_V^*)$
Fisher	− 3.41	0.535	39	2.30×10^{-115}
Bankoff	− 3.81	0.478	28	3.56×10^{-94}
Bernath	− 2.35	0.765	160	6.12×10^{-246}

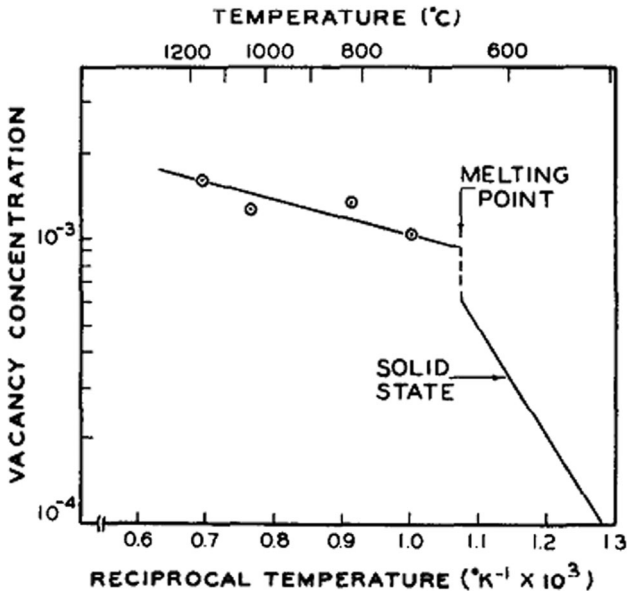

Fig. 7—Relationship between vacancy concentration and temperature[81] (Work done for US Government, no copyright).

discussed. Fisher[67] studied heterogeneous nucleation of a pore at the interface between a solid substrate and a liquid by assuming a shape bounded by a plane and a portion of a spherical surface, as presented in Figure 10 (a), where σ_{LP}, σ_{PO}, and σ_{LO} represent the liquid–pore, solid–pore, and solid–liquid surface tensions, respectively. Fisher showed that the fracture pressure at the interface where the pore has an angle θ with the solid substrate, is reduced by a factor:

$$\frac{\Delta P^*_{het}}{\Delta P^*_{hom}} = \sqrt{\frac{(2-\cos\theta)(1+\cos\theta)^2}{4}} \qquad [15]$$

As θ approaches 180 deg, *i.e.*, perfect non-wetting substrate, the fracture pressure of heterogeneous nucleation goes to zero. However, θ → 180 deg is unrealistic and according to Campbell,[102] the maximum contact angles ever observed, based on a survey of several dozen researches, appeared to approach an upper limit of approximately 160 deg. At $\theta = 160$ deg, Eq. [15] yields 0.05. Therefore the fracture pressure for heterogeneous nucleation in liquid aluminum falls between − 191 and − 118 MPa. These values are still much higher than the ones assumed in the literature and the tensile strength of

Table III. Fracture Pressure, Critical Radius, and Vacancy Cluster Size Recalculated by Taking Curvature Effects into Account

Equations	ΔP^*(GPa)	r^* (nm)	n^*
Fisher	− 3.31	0.539	40
Bankoff	− 3.66	0.484	29
Bernath	− 2.35	0.776	160

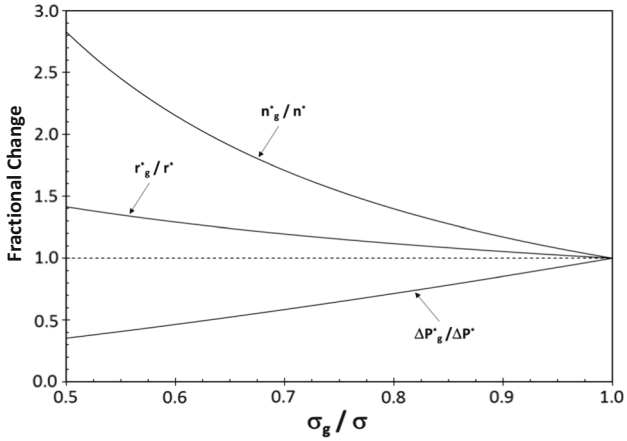

Fig. 8—The effect of change in surface energy on fracture pressure, critical pore size, and number of vacancies needed for the pore to be stable.

pure aluminum and aluminum alloys reported at melting temperature.

Chalmers[104] stated that the work of formation of an embryonic pore is reduced on a concave substrate, and Fisher[67] speculated that it may become zero for perfectly sharp notches. Hence, pore nucleation in a perfectly sharp notch corresponds to the nucleation of a crack in the solid inclusion. There are good reasons for believing that, similar to the nucleation of pores in liquids not being possible, the nucleation of cracks in solids is also impossible.[105] Bankoff[68] considered the growth and emergence of the embryo from re-entrant angles. Although nucleation may occur easily at the root of the notch, the growth of the resulting pore will be arrested at the notch entrance because the pore radius must exceed the critical size with respect to the bulk of the liquid. Based on this, although an inclusion may increase the probability of pore nucleation, it is not possible to attribute the pores in aluminum castings to heterogeneous pore nucleation. Therefore nucleation of pores in solidifying aluminum, either homogeneously or heterogeneously, is impossible.

VI. RECONCILIATION OF OBSERVATIONS, CALCULATIONS, AND ASSUMPTIONS

If pores cannot nucleate in liquid aluminum either homogeneously or heterogeneously, how can the prevalence of pores in aluminum castings be explained? Although pores cannot nucleate in liquid aluminum, there is a mechanism by which pores can grow, without nucleation. Campbell[102] stated that the entrainment of the surface oxides to form double parallel oxide films (bifilms) may act as initiation sites and subsequently, they can easily open up by pressure of dissolved gas. This point is supported by the findings of Fox and Campbell[106] who conducted an experiment in which a reduced pressure test sample was observed *via* real-time X-ray radiography under different pressure levels. Two radiographs taken at a pressure of 1.0 and 0.01 atmosphere during this experiment are presented in Figure 11. At 1.0 atm, there are no visible pores, however, there are numerous dark patches. When pressure is reduced, the dark patches, which are bifilms in their compact, convoluted state, open up under the expansion of entrained air (residual gases, hydrogen and argon) between the two layers of the oxide. Hence pores form without any nucleation, and only through growth of the bifilms, at only modest reduced pressures of almost 1 atm, consistent with the assumptions for fracture pressure levels presented in Table I. Similarly, the *in situ* observations summarized previously show growth of pores, even when the bulk and local solid fractions are well below the levels required for pore nucleation. For pores to form under such conditions, where nucleation is impossible, the only viable mechanism is the opening up of folded-over films entrained by turbulence (bifilms). Hence, the presence of bifilms entrained is the sole mechanism underlying pore formation. In the presence of bifilms, nucleation is completely bypassed because fracture of the liquid under pressure is no longer needed due to the crack-like nature of bifilms. To the authors' knowledge, this effect of bifilms, *i.e.*, bypassing nucleation, has not been highlighted previously. This explanation is in complete agreement with the *in situ* observations, as well as the pressure assumptions presented in Table I. The initial growth of pores in relatively large, enveloping bifilms might display a series of spherical forms if the bifilm is mechanically weak as a result of its thinness. In contrast, irregular forms may result because of the mechanical constraint of thicker, more rigid bifilms. However, if bifilms are much smaller in size, as would be expected from fresh, "young" oxides that become "chopped" during mold filling, it is conceivable that a pore would initially form by opening the bifilm, but then grow beyond the size of the bifilm as a substantial sphere expanding freely in the liquid, as also observed during *in situ* experiments. The presence of oxides on the walls of pores has been confirmed recently.[2,107–109]

If nucleation of pores is not possible, one may ask how the hydrogen rejected from solidifying aluminum would be accommodated in the absence of oxide films. It is well known that hydrogen and vacancies have a high binding energy[110–112] and a vacancy in aluminum is capable to trapping up to twelve hydrogen atoms.[113] Therefore hydrogen supersaturation, assumed in the literature to drive pore nucleation upon solidification of aluminum can be easily accommodated by the solid equilibrium vacancy concentration, shown in Figure 7. Hence, the assumption usually made in the literature that hydrogen necessarily precipitates during solidification, because of the abrupt change in hydrogen solubility, is not well founded.

With the insights provided in this study, we can turn our attention back to certain points raised earlier in the paper:

1. The final shape of the pores does not necessarily indicate the root cause of pore initiation. In Figure 1, the presence or otherwise of dendrites merely indicates the timing of the growth of the

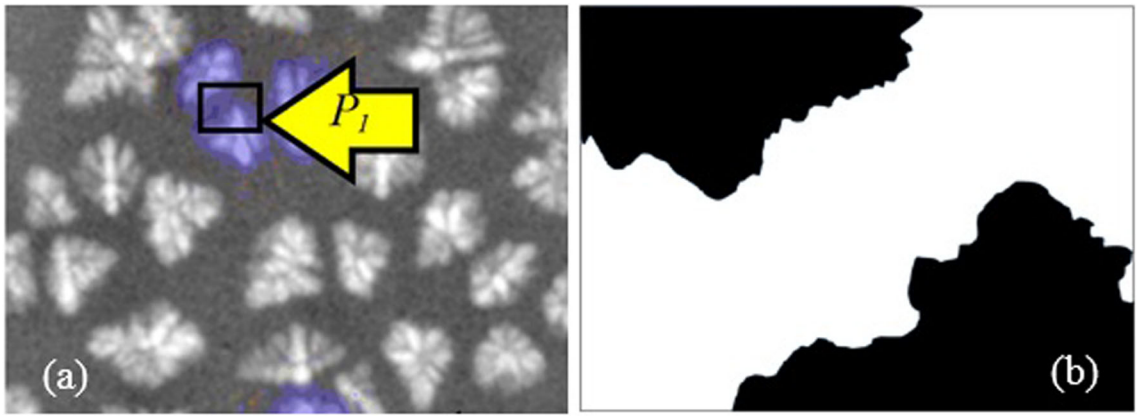

Fig. 9—(*a*) The vicinity of the first pore in experiments by Murphy *et al*. and (*b*) the digital version for image analysis of the area in the box.

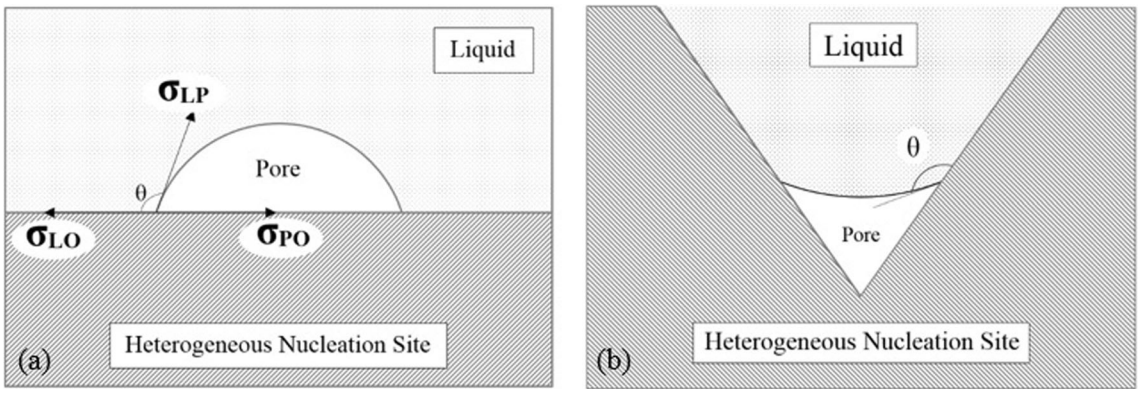

Fig. 10—Heterogeneous nucleation of a pore at various interfaces: (*a*) nucleation on a plane surface, (*b*) nucleation on concave substrate.

pore; if early, it will be round, whether pore growth is driven by shrinkage or gas because the pore will grow freely in the liquid. However, if the pore forms late during solidification, it will exhibit cusps (again, whether shrinkage or gas driven) as a result of impingement on surrounding dendrites. Examples are provided in Reference 102 in Figures 7.46 and 7.47, which show subsurface pores around a core. All pores are in the same hydrogen diffusion field from the reaction with the core binder, but adjacent pores are dendritic or round randomly. This has to be the result of very different ease of unfurling of randomly furled bifilms.

2. Note in Figure 5 that some pores smaller than 1 mm are not spherical. Pores smaller than about 1 mm diameter become increasingly like spherical bullets as their size diminishes; they become mechanically very hard and undeformable as a result of their diminishing radius of curvature. Thus all small pores should be expected to be perfectly round. If not, some important factor must be influencing their shape. Consequently, pores in Figure 5 can be attributed to bifilms opening during the last stages of solidification. Pores may be forming on raveled bifilms, in which case part of the bifilm will open easily and quickly, and therefore likely to create a small spherical pore, but the remainder of the bifilm only unfurls slowly, to form a fairly linear pore, or fairly linear array of small pores. The evidence for such a process has been presented by Tynelius and Major[114] and later by Campbell[1] who reinterpreted their results. The degree of unfurling of the bifilm is determined by the drive for growth, *i.e*., gas content and local solidification time (as determined by dendrite arm spacing), the latter of which can be also taken as an indication of negative pressure due to shrinkage of the metal around an internal pore.
3. The assumptions made in pore formation models in aluminum castings, summarized in Table II, were coupled with growth and solidification equations to give good results compared to experimental data. These assumptions for pore nucleation, *i.e*., fracture pressure (0.1 MPa) and critical pore size ($\lambda_{DA}/2$), can only be valid if the bifilm theory is applied, which states that there are preexisting unbonded surfaces, *i.e*., bifilms, already in the liquid metal.
4. Bifilms are extrinsic defects that form due to entrainment of surface oxide films. Consequently, the statements made in the literature that pores in castings are intrinsic are not accurate.

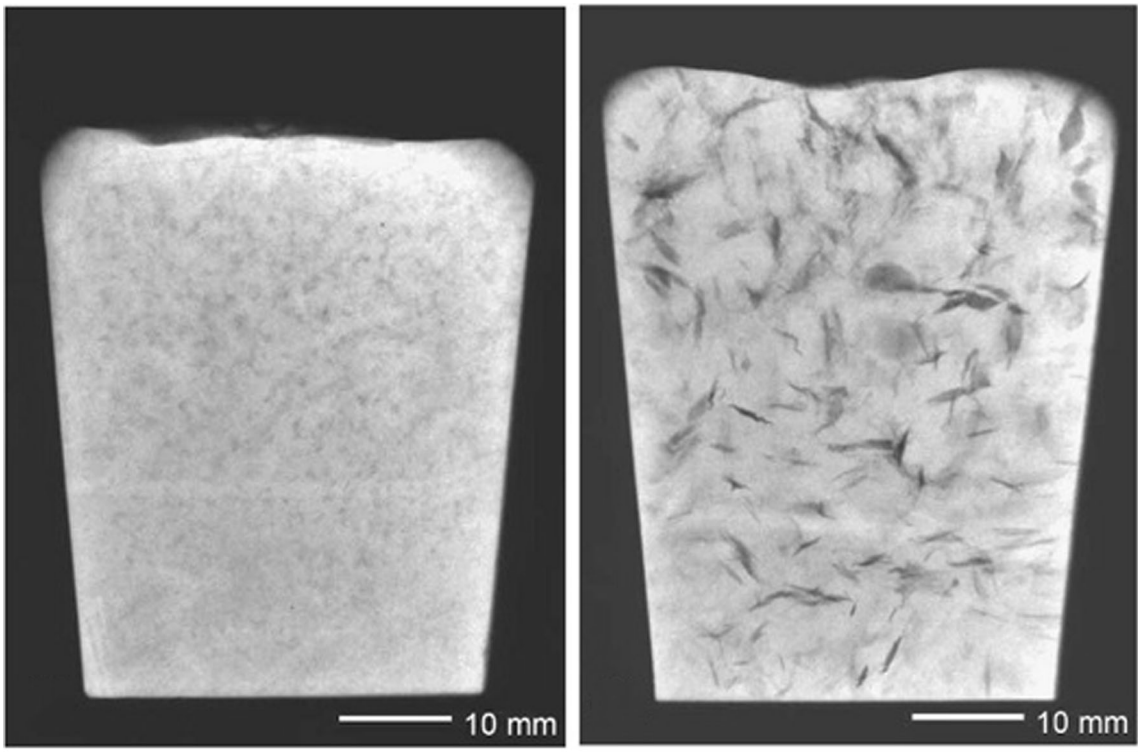

Fig. 11—Radiographs of reduced pressure test samples of the same as-melted Al-7Si-0.4Mg alloy solidified; (*a*) Under pressure of 1 atm., (*b*) Under pressure of 0.01 atm. (From ***Ref. [106] with permission).

VII. CONCLUSIONS

1. Calculations for fracture pressure, critical pore size, and probability of formation of a vacancy cluster at or above the critical size, based on classical nucleation theory, showed that homogeneous nucleation of a pore in solidifying aluminum is impossible.
2. Assumption commonly made in the literature that pores form only in the last stages of solidification when solid fraction and local hydrogen supersaturation are high is not accurate. Examples of *in situ* observations from the literature showed that pore may nucleate (i) far from the solidification front where hydrogen supersaturation has not occurred yet, and (ii) at a low solid fraction.
3. The review of the literature along with calculations showed that for heterogeneous nucleation, (i) a substrate with low wetting condition needs to be present in liquid aluminum, (ii) the fracture pressure for heterogeneous nucleation on the most favored (least wetted surface) is two orders of magnitude higher than experimental tensile strengths for solidifying aluminum alloys. Therefore, heterogeneous nucleation is not possible.
4. As opposed to statements made in the literature, pores are not intrinsic but extrinsic defects. Therefore they can be eliminated.
5. The only mechanism available for pore formation in solidifying aluminum is the presence of bifilms, which can inflate due to reduced pressure and/or hydrogen segregation. Therefore, pore formation does not involve nucleation, it is a pure growth process.
6. The bifilm theory appears to be completely consistent with *in situ* observations and assumptions commonly made in the casting/solidification literature.

CONFLICT OF INTEREST

The authors declare that they have no conflict of interest.

NOMENCLATURE

α	Atomic packing factor
θ	Wetting angle
ΔG_0	Free energy of activation for the motion of an individual molecule of liquid past its neighbors into or away from the pore surface (J)
ΔP	Pressure difference between the exterior and the interior of the pore (GPa)
λ_{DA}	Dendrite arm spacing (μm)
σ	Bulk surface energy per unit area (J/m^2)
σ_{eff}	Effective surface energy (J/m^2)
σ_{LP}	Liquid–pore surface energy (J/m^2)
σ_{LO}	Liquid–solid surface energy (J/m^2)

σ_{PO}	Pore–solid surface energy (J/m^2)
γ	Curvature energy (N)
ρ	Density (kg/m^3)
C_{AP}	Atomic packing factor
c_v	Vacancy concentration
E_n	Formation energy of a spherical cluster of vacancy (J)
E_v	Formation energy of a vacancy (J)
f_S	Solid fraction
F	Probability
P	Pressure (GPa)
h	Planck's constant (J s)
H_V	Molecular heat of vaporization (J)
J_0	Nucleation rate factor (s^{-1})
J	Nucleation rate (s^{-1})
k	Boltzmann's constant ($J\ K^{-1}$)
M	Molar mass (kg/mol)
n	Number of atoms/vacancies
N_A	Avogadro's number (mol^{-1})
r	Radius of nuclei/atoms/vacancies (nm)
T	Temperature (K)
V	Volume (m^3)
W	Work (J)
W_s	Required energy to form a vacancy cluster containing n vacancies in the absence of gas (J)

SUBSCRIPTS

*	Critical
A	Atom
atm	Atmosphere
e	External
g	Gas
H	Hydrostatic
Het	Heterogeneous
Hom	Homogeneous
l	Liquid
s	Shrinkage
V	Vacancy

REFERENCES

1. J. Campbell: *Mater. Sci. Technol.*, 2006, vol. 22 (2), pp. 127–45.
2. N.R. Green and J. Campbell: *Mater. Sci. Eng. A*, 1993, vol. 173 (1), pp. 261–66.
3. C. Nyahumwa, N.R. Green, and J. Campbell: *Metall. Mater. Trans. A*, 2001, vol. 32A (2), pp. 349–58.
4. M. Tiryakioğlu, J. Campbell, and J.T. Staley: *Mater. Sci. Eng. A*, 2004, vol. 368 (1–2), pp. 205–11.
5. M. Tiryakioğlu, J. Campbell, and J.T. Staley: *Scr. Mater.*, 2003, vol. 49 (9), pp. 873–78.
6. M. Tiryakioğlu: *Mater. Sci. Eng. A*, 2010, vol. 527 (18–19), pp. 4546–49.
7. B.G. Eisaabadi *et al.*: *Mater. Sci. Eng. A*, 2013, vol. 579, pp. 64–70.
8. M. Tiryakioğlu, J.T. Staley, and J. Campbell: *Mater. Sci. Eng. A*, 2008, vol. 487 (1–2), pp. 383–87.
9. M. Tiryakioğlu, J.T. Staley, and J. Campbell: *Mater. Sci. Eng. A*, 2004, vol. 368 (1), pp. 231–38.
10. M. Tiryakioğlu, J. Campbell, and N.D. Alexopoulos: *Metall. Mater. Trans. A*, 2009, vol. 40A (4), pp. 1000–07.
11. M. Tiryakioğlu, J. Campbell, and N.D. Alexopoulos: *Mater. Sci. Eng. A*, 2009, vol. 506 (1), pp. 23–26.
12. M. Tiryakioğlu and J. Campbell: *Int. J. Metalcast.*, 2014, vol. 8 (3), pp. 39–42.
13. M. Tiryakioclu and J. Campbell: *Mater. Sci. Technol.*, 2009, vol. 25 (6), pp. 784–89.
14. J.T. Staley, Jr, M. Tiryakioğlu, and J. Campbell: *Mater. Sci. Eng. A*, 2007, vol. 465 (1), pp. 136–45.
15. H. Özdeş and M. Tiryakioğlu: *J. Mater. Eng. Perform.*, 2017, vol. 26 (2), pp. 736–43.
16. M. Tiryakioğlu, J. Campbell, and C. Nyahumwa: *Metall. Mater. Trans. B*, 2011, vol. 42B (6), pp. 1098–1103.
17. M. Tiryakioğlu: *Mater. Sci. Eng. A*, 2009, vol. 520 (1), pp. 114–20.
18. M. Tiryakioğlu: *Metall. Mater. Trans. A*, 2009, vol. 40A (7), pp. 1623–30.
19. M. Tiryakioğlu: *Metall. Mater. Trans. A*, 2015, vol. 46A (1), pp. 270–80.
20. I. Farup, J.-M. Drezet, and M. Rappaz: *Acta Mater.*, 2001, vol. 49, pp. 1261–69.
21. T.C. Piwonka and M.C. Flemings: *Trans. Metall. Soc. AIME*, 1966, vol. 236, pp. 1157–65.
22. G. Timelli, and D. Caliari: in Shape Casting: 6th International Symposium, M. Tiryakioğlu, M. Jolly, and G. Byczynski, Springer, Cham, 2016, pp. 151–58.
23. L. Katgerman, D.G. Eskin.: in Hot Cracking Phenomena in Welds II, H.H.T. Bollinghaus, C.E. Cross, J.C. Lippold, Springer, Berlin, 2008, pp. 3–18.
24. A. Nazarboland and R. Elliott: *Int. J. Cast Met. Res.*, 1997, vol. 10 (2), pp. 87–97.
25. J. Anson, M. Stucky, and J. Gruzleski: *Trans. Am. Foundrymen's Soc.*, 2000, vol. 108, pp. 419–26.
26. K.A. Jackson and J.D. Hunt: *Acta Metall.*, 1965, vol. 13 (11), pp. 1212–15.
27. Q. Han: *Scr. Mater.*, 2006, vol. 55 (10), pp. 871–74.
28. W.C. McCrone: *Fusion Methods in Chemical Microscopy*, Interscience Publishers, Geneva, 1957.
29. E.M. Chamot and C.W. Mason: *Handbook of Chemical Microscopy*, Wiley, Hoboken, 1958.
30. J.D. Hunt, K.A. Jackson, and H. Brown: *Rev. Sci. Instrum.*, 1966, vol. 37 (6), p. 805.
31. W.F. Kaukler: *Rev. Sci. Instrum.*, 1984, vol. 55 (10), pp. 1643–47.
32. P.D. Lee and J.D. Hunt: *Acta Mater.*, 1997, vol. 45 (10), pp. 4155–69.
33. L. Arnberg and R.H. Mathiesen: *JOM*, 2007, vol. 59 (8), pp. 20–26.
34. H. Yin and J.N. Koster: *ISIJ Int.*, 2000, vol. 40 (4), pp. 364–72.
35. A.V. Catalina, S. Sen, D.M. Stefanescu, and W.F. Kaukler: *Metall. Mater. Trans. A*, 2004, vol. 35A (5), pp. 1525–38.
36. A. Murphy, D. Browne, Y. Houltz and R. Mathiesen: *IOP Conference Series: Materials Science and Engineering*, IOP Publishing, Bristol, 2016.
37. Z. Lei, L. Hengcheng, P. Ye, W. Qigui, and S. Guoxiong: In-situ Observation of Porosity Formation During Directional Solidification of Al-Si Casting Alloys, Research & Development, 2011.
38. E. Kato: *Metall. Mater. Trans. A*, 1999, vol. 30A (9), pp. 2449–53.
39. M. Volmer and A. Weber: *Z. Phys. Chem.*, 1926, vol. 119, pp. 277–301.
40. M. Volmer: Kinetics of Phase Formation, Air Force Cambridge Research Center, Geophysics Research Division, Atmospheric Physics Laboratory, Cambridge, MA, 1940.
41. R. Becker and W. Döring: *Ann. Phys.*, 1935, vol. 416 (8), pp. 719–52.
42. J.W. Gibbs, H.A. Bumstead, and R.G. Van Name: Scientific Papers of J. Willard Gibbs …: Thermodynamics, Scientific Papers of J. Willard Gibbs, Longmans, Green and Company, 1906.
43. J.H. Hollomon and D. Turnbull: *Prog. Met. Phys.*, 1953, vol. 4, pp. 333–88.
44. J.P. Hirth and G.M. Pound: *Condensation and Evaporation: Nucleation and Growth Kinetics*, Macmillan, Basingstoke, 1963.
45. J.P. Hirth, G.M. Pound, and G.R. St. Pierre: *Metall. Trans.*, 1970, vol. 1 (4), pp. 939–45.
46. F.G. Blake: The Tensile Strength of Liquids a Review of the Literature, Acoustics Research Laboratory, Department of Engineering Sciences and Applied Physics, Harvard University, Cambridge, MA, 1954.
47. J. Frenkel: *Kinetic Theory of Liquids*, Dover Publications, Dover, 1955, pp. 174–82.

48. J.A. Clark: *The Thermodynamics of Bubbles*, MIT, Cambridge, MA, 1956.
49. S.F. Jones, G.M. Evans, and K.P. Galvin: *Adv. Colloid Interface Sci.*, 1999, vol. 80 (1), pp. 27–50.
50. P.D. Lee, A. Chirazi, and D. See: *J. Light Met.*, 2001, vol. 1 (1), pp. 15–30.
51. C. Pequet, M. Rappaz, and M. Gremaud: *Metall. Trans. A*, 2002, vol. 33 (7), pp. 2095–2106.
52. K. Kubo and R.D. Pehlke: *Metall. Trans. B*, 1985, vol. 16 (2), pp. 359–66.
53. I. Katzarov and J. Popov: *Int. J. Heat Mass Transfer*, 1996, vol. 39 (14), pp. 2861–67.
54. D.R. Poirier, K. Yeum, and A.L. Maples: *Metall. Trans. A*, 1987, vol. 18 (11), pp. 1979–87.
55. Q.T. Fang, and D.A. Granger: Prediction of pore size due to rejection of hydrogen during solidification of aluminum alloys.
56. I.J. Chiou and H.L. Tsai: *AFS Trans.*, 1990, vol. 98, pp. 823–30.
57. J.D. Zhu, and I. Ohnaka: Model. Cast., Weld. Adv. Solidif. Process. V, Proc. Int. Conf. 1991. Vol. V. pp. 435–42.
58. P.D. Lee, D. See, and R.C. Atwood: Cutting Edge of Computer Simulation of Solidification and Casting. 1999. pp. 97–111.
59. P.D. Lee, R.C. Atwood, R.J. Dashwood, and H. Nagaumi: *Mater. Sci. Eng. A*, 2002, vol. 328 (1), pp. 213–22.
60. P.D. Lee, and J.D. Hunt: Conference: 7. Model. Cast., Weld. Adv. Solidif. Processes. London. 10–15 Sep 1995.
61. J.G. Conley, J. Huang, J. Asada, and K. Akiba: *Mater. Sci. Eng. A*, 2000, vol. 285 (1–2), pp. 49–55.
62. J. Huang, J.G. Conley, and T. Mori: *Metall. Mater. Trans. B*, 1998, vol. 29B (6), pp. 1249–60.
63. R.C. Atwood, S. Sridhar, W. Zhang, and P.D. Lee: *Acta Mater.*, 2000, vol. 48 (2), pp. 405–17.
64. D.M. Stefanescu: *Int. J. Cast Met. Res.*, 2005, vol. 18 (3), pp. 129–43.
65. D.M. Stefanescu and A.V. Catalina: *Int. J. Cast Met. Res.*, 2011, vol. 24 (3–4), pp. 144–50.
66. J.C. Fisher, J.H. Hollomon, and D. Turnbull: *J. Appl. Phys.*, 1948, vol. 19 (8), p. 775.
67. J.C. Fisher: *J. Appl. Phys.*, 1948, vol. 19 (11), pp. 1062–67.
68. S.G. Bankoff: *Trans. ASME*, 1957, vol. 79, pp. 735–40.
69. L. Bernath: *Ind. Eng. Chem.*, 1952, vol. 44 (6), pp. 1310–13.
70. W.F. Gale and T.C. Totemeier: *Smithells Metals Reference Book*, Butterworth-Heinemann, Oxford, 2003.
71. T. Bazhirov, G. Norman, and V. Stegailov: *J. Phys.: Condens. Matter*, 2008, vol. 20 (11), pp. 113–14.
72. Z. Insepov, A. Hassanein, T.T. Bazhirov, G.Ã. Norman, and V. V. Stegailov: *Fusion Sci. Technol.*, 2007, vol. 52 (4), pp. 885–89.
73. P. Yousefian and M. Tiryakioğlu: *Defects and Properties of Cast Metals (TMS 2017)*, San Diego, California, 2017.
74. M.M. Martynyuk: *J. Eng. Phys. Thermophys.*, 1999, vol. 72 (4), pp. 682–86.
75. H. Fredriksson, M. Haddad-Sabzevar, K. Hansson, and J. Kron: *Mater. Sci. Technol.*, 2005, vol. 21 (5), pp. 521–30.
76. S.J. Zinkle, L.E. Seitzman, and W.G. Wolfer: *Philos. Mag. A*, 1987, vol. 55 (1), pp. 111–25.
77. H. Brooks: *Impurities and Imperfections*, ASM Seminar, Ohio, 1955.
78. K.A. Jackson: *Philos. Mag.*, 1962, vol. 7 (79), pp. 1117–27.
79. G. Thomas and R.H. Willens: *Acta Metall.*, 1964, vol. 12 (2), pp. 191–96.
80. G. Thomas and R.H. Willens: *Acta Metall.*, 1966, vol. 14 (10), pp. 1385–90.
81. G. Thomas, and R. Willens: Defects in Aluminum Quenched from the Liquid State, DTIC Document, 1963.
82. D. Kuhlmann-Wilsdorf and H.G.F. Wilsdorf: *J. Appl. Phys.*, 1960, vol. 31 (3), pp. 516–25.
83. J.P. Perdew, Y. Wang, and E. Engel: *Phys. Rev. Lett.*, 1991, vol. 66 (4), pp. 508–11.
84. J.A. Sigler and D. Kuhlmann-Wilsdorf: *Phys. Status Solidif. B*, 1967, vol. 21 (2), pp. 545–56.
85. M.R. Mruzik and K.C. Russell: *Surf. Sci.*, 1977, vol. 67 (1), pp. 205–25.
86. A. Si-Ahmed, and W. Wolfer: Am. Soc. Test. Mater., Spec. Tech. Publ., 782(CONF-820628-), 1982.
87. C. Ransley and H. Neufeld: *J. Inst. Met.*, 1948, vol. 74 (12), pp. 599–620.
88. W. Eichenauer: *Z. Metall.*, 1968, vol. 59 (8), pp. 613–16.
89. S.J. Zinkle, W.G. Wolfer, G.L. Kulcinski, and L.E. Seitzman: *Philos. Mag. A*, 1987, vol. 55 (1), pp. 127–40.
90. S. Yoshiharu and M. Yoshijiro: *Jpn. J. Appl. Phys.*, 1981, vol. 20 (10), p. 1787.
91. K. Watanabe, Y. Morishita, H. Yamaguchi, and S. Yoshida: *Jpn. J. Appl. Phys.*, 1981, vol. 20 (10), p. 1791.
92. M. Kiritani: *J. Phys. Soc. Jpn.*, 1964, vol. 19 (5), pp. 618–31.
93. G. Das and J. Washburn: *Philos. Mag.*, 1965, vol. 11 (113), pp. 955–67.
94. A. Chaudhuri, M.A. Singh, B.J. Diak, C. Cuoppolo, and A.R. Woll: *Philos. Mag.*, 2013, vol. 93 (35), pp. 4392–4411.
95. E.D. Hondros: *Acta Metall.*, 1968, vol. 16 (11), pp. 1377–80.
96. C. Bauer, R. Speiser, and J. Hirth: *Metall. Mater. Trans. A*, 1976, vol. 7A (1), pp. 75–79.
97. M.F. Felsen and P. Regnier: *Surf. Sci.*, 1977, vol. 68, pp. 410–18.
98. I.F. Bainbridge and J.A. Taylor: *Metall. Mater. Trans. A*, 2013, vol. 44 (8), pp. 3901–09.
99. I. Egry, E. Ricci, R. Novakovic, and S. Ozawa: *Adv. Colloid Interface Sci.*, 2010, vol. 159 (2), pp. 198–212.
100. F.A. Halden and W.D. Kingery: *J. Phys. Chem.*, 1955, vol. 59 (6), pp. 557–59.
101. D. Sageman: *Surface Tension of Molten Metals Using the Sessile Drop Method*, Ames Lab, Iowa, 1972.
102. J. Campbell: *Complete Casting Handbook: Metal Casting Processes, Metallurgy, Techniques and Design*, Elsevier Butterworth-Heinemann, Oxford, 2011.
103. E. Whittenberger and F. Rhines: *J. Met.*, 1952, vol. 7, pp. 409–20.
104. B. Chalmers: Principles of solidification, in Applied Solid State Physics, W. Low, and M. Schieber, 1970, Springer, Boston, MA, pp. 161–70.
105. J. Campbell: *Metall. Mater. Trans. B*, 2011, vol. 42B (6), pp. 1091–97.
106. S. Fox and J. Campbell: *Scr. Mater.*, 2000, vol. 43 (10), pp. 881–86.
107. D. Mackie, J.D. Robson, P.J. Withers, and M. Turski: *Mater. Charact.*, 2015, vol. 104, pp. 116–23.
108. A. Shafaei and R. Raiszadeh: *Metall. Mater. Trans. B*, 2014, vol. 45B (6), pp. 2486–94.
109. M. Tang and P.C. Pistorius: *Int. J. Fatigue*, 2017, vol. 94 (Part 2), pp. 192–201.
110. Y. Fukai and N. Okuma: *Jpn. J. Appl. Phys.*, 1993, vol. 32 (9A), p. L1256.
111. H.K. Birnbaum, C. Buckley, F. Zeides, E. Sirois, P. Rozenak, S. Spooner, and J.S. Lin: *J. Alloys Compd.*, 1997, vol. 253, pp. 260–64.
112. A.I. Kartamyshev, D.D. Vo, and A.G. Lipnitskii: *St. Petersb. Polytech. Univ. J. Phys. Math.*, 2016, vol. 2 (2), pp. 96–102.
113. G. Lu and E. Kaxiras: *Phys. Rev. Lett.*, 2005, vol. 94 (15), p. 155501.
114. K. Tynelius, J. Major, and D. Apelian: *Trans. Am. Foundrymen's Soc*, 1993, vol. 101, pp. 401–13.
115. K.D. Carlson, Z. Lin, and C. Beckermann: *Metall. Trans. B*, 2007, vol. 38 (4), pp. 541–55.